Australian Journal of Basic and Applied Sciences, 7(7): 613-622, 2013
ISSN 1991-8178

Temperature Effects on Curved Stationary Viscous Thermal Fiber Jets

Dhanya V. Mukundan, Satyananda Panda

Department of Mathematics National Institute of Technology, Calicut, NIT P.O – 673601, Calicut, Kerala, India.

Abstract: Centrifugal fiber spinning process is an important industrial process for the production of fibers or wools. This study is an attempt to understand and analyze the effect of temperature in the centrifugal spinning process. The work deals with the mathematical modeling and numerical simulations of the dynamics of curved non-isothermal Newtonian fibers, which is practically applicable to the description of centrifugal spinning process of glass wool or glass fibers. The involved quantities in the model are the fiber cross-sectional area, fluid velocity, tension, temperature and the coordinates of the fiber center-line. In this work we restrict ourselves to the stationary case. The effects of temperature-dependent viscosity, gravity, surface tension, as well as those of axial heat conduction, heat convection and radiative heat transfer are taken into account. For the numerical simulation of the model equations, finite volume scheme on a uniform staggered grid is used. Numerical results for the fiber radius, axial velocity and temperature are shown, illustrating the cooling effects of Stanton, Peclet and radiation numbers.

Key words: Centrifugal spinning process, Stanton number, Peclet number, Reynolds number, Rossby number

INTRODUCTION

Studies on the dynamics of viscous fibers are motivated by a wide range of applications in the industry of spinning and drawing of polymer or glass fibers. History shows that the existing works are mostly related to the fiber draw-down process in the context of flow of straight, slender viscous fibers. A great deal of the literature concerns fiber-drawing models that are essentially small perturbations about prescribed steady unidirectional extensional flows. Various studies have considered the additional effects of, heat transfer (Glickman, 1968), inertia (Shah *et al*., 1972) and surface tension (Cummings *et al*., 1999), unsteadiness (Forest *et al*., 2001). The effects of both gravity and inertia were included in a general theory of slender viscous fibers of arbitrary cross section (Dewynne *et al*., 1994). Fiber spinning is also well discussed in the literature. Because of the large elongations seen in these types of flow a slenderness assumption is also possible, leading to an approximate one-dimensional theory. The unsteady system of viscous-dominated fibers was first given in (Kase *et al*., 1965) and the full system is given in (Matovich *et al*., 1969). Also the steady system is derived systematically in (Schultz *et al*., 1982) from the axisymmetric equations of motion. Dewynne *et al*., (1989) proposed an asymptotic model of fiber drawing that was essentially similar to (Geyling, 1976), but showed that, unless the initial conditions possess certain singularities, the cross-sectional area cannot be made to vanish in finite time. There exist numerous other research works on straight fibers in connection with stability and breakup (see e.g. Kate, 1991, Eggers, 1997). Drawing of viscous sheets, as in the manufacture of sheet glass (Doyle, 1994) is quite similar to fiber spinning. There exist lots of literatures about the cooling effects on fibers in the context of straight fibers. Bourne and Dixon (1971) used integral solutions for the cooling fiber, neglecting resistance within the fiber and using averaged values of fluid properties. Their results showed good agreement with experimental measurements by Arridge and Prior (1964) on 15 to 50μm diameter on glass fibers. They showed that attention to the averaging of temperature-dependent air properties was quite important. Chida and Katto (1976) subsequently amended the Bourne and Dixon theory to account for radial heat conduction in the fibers; for conditions typical of glass fibers, radial conduction proves to be negligible. Maddison and McMillan (1978) reported further experiments on fiber cooling which were in general agreement with the results of Arridge and Prior (1964). Huynh and Tanner (1983) studied the non-isothermal glass fiber drawing process using a two-dimensional finite-element method. Gupta and Schultz (1998) have analyzed steady, non-isothermal Newtonian fiber drawing. Bechtel *et al*. (1992) and Wang and Forest (1994) study the non-isothermal fiber drawing process of a viscoelastic fluid based on a Maxwell model.

Corresponding Author: Dhanya V. Mukundan, Department of Mathematics National Institute of Technology, Calicut, NIT P.O – 673601, Calicut, Kerala, India.
E-mail: dhanyavmukundan@nitc.ac.in,

The origin of present study lies in the rotary spinning process and our applications concentrate on the glass wool production in the centrifugal spinning process. Glass wool that is produced by a centrifugal spinning process is mostly used for the thermal insulation in homes and buildings, and it is of increasing industrial importance. In this process, centrifugal forces press hot molten glass through small nozzles of a rapidly rotating cylindrical drum. The molten glass streams are converted into fibers by a downward blast of air, hot gas, or both. Fibers are produced with an average length less than one meter due to the breakage. Finally the fibers fall onto a conveyor belt, where they interlace with each other in a fleecy mass. A schematic drawing of the production process is given in Fig. 1. This can be used for insulation, or the wool can be sprayed with a binder, compressed into the desired thickness, and cured in an oven. The heat sets the binder, and the resulting product may be a rigid or semi-rigid board, or a flexible batt. A study of rotary spinning requires understanding of the behavior of the fibers between the nozzle at the spinneret and conveyor belt.

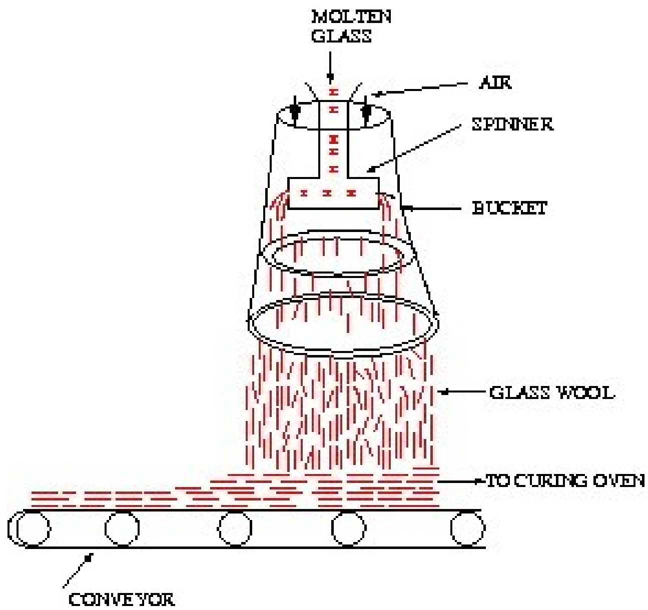

Fig. 1: A schematic diagram of the centrifugal spinning process.

Although there has been quite a lot research on the development of one-dimensional mathematical models for the analysis of straight fibers and jets under isothermal and non-isothermal conditions, curved fibers such as those related to rotary spinning process have received very little attention due to its complex geometry. Spiraling liquid jets (a 2D jet under the influence of centrifugal and Coriolis forces and surface tension), and jets curved by gravity are extensively studied with the focus on instabilities and droplet formation. For such curved, coiled flows one dimensional model equations were derived from the stationary assumption and considering the flow as uniaxial, see (Decent, 2002 & 2004, Wallwork, 2002, Kolk, 2005). Jets in 3D under the influence of gravity or centrifugal and Coriolis forces are studied by many authors. The uniaxial and curved stationary approaches of Decent *et al.* (2002) have been generalized by Panda *et al.* (2007 & 2008) for the systematic derivation of an asymptotic model for the dynamics of curved isothermal viscous fiber neglecting surface tension. As an extension of these Marheineke *et al.* (2009) included the surface tension effect in the fiber model thereby deduced the boundary condition for the free fiber end. Also recently A. Hlod *et al.* (2009) had a detailed study on the steady jet model in rotary spinning process. Previous studies on curved fibers have mainly considered isothermal flows of either Newtonian or non-Newtonian fluids. Therefore our interest is to study steady single thermal fiber. We focus on the numerical simulations of the steady curved non-isothermal Newtonian incompressible fibers. We use slender body theory and extend the work of (Marheineke *et al.*, 2009) to non-isothermal flow. The model accounts for the effects of inertial, viscous, and external body forces (centrifugal and coriolis forces) with temperature effects. We neglect air drag, this allows us to avoid considering possible instabilities caused by these effects. Moreover this work highlights the role of cooling effects on the fiber dynamics in the centrifugal spinning process.

In the stationary fiber problem the fiber center-line and the dependent variables like velocity, cross-sectional area, etc. as well as boundary conditions are independent of time. However, one can also simulate a time dependent fiber model for the generation of the fiber for a long time and then asymptotically reach steady-state with stationary boundary conditions. For the analysis of the steady-state we must consider a fiber of infinite length, which is unlike in reality, where the fiber breaks at a certain point and is thus limited to a finite length. Hence, only a part of the fiber needs to be considered for the discussion of the stationary problem. This means that the shape of the fiber and the dependent variables will be observed for a finite fiber length only. In the light of these discussions it is useful to study the steady-state fiber model. The method is based on one-dimensional equations of motion of the curved fiber in which the effects of the temperature-dependent viscosity, gravity and surface tension are taken into account. These equations are coupled by heat transfer equation for the temperature profile in the fiber, accounting for the effects of the axial heat conduction, heat convection and radiative heat transfer. Selected numerical results are shown to demonstrate the role of cooling effects based on Stanton, Peclet and radiation numbers.

Governing equations:

The fiber fluid is considered as a non-isothermal Newtonian with constant values of density ρ, the specific heat capacity C_ρ, the heat transfer coefficient α_h and the coefficient of surface tension σ. Also the coefficient of viscosity μ is considered as temperature dependent, a non-linear dependence of dynamic viscosity law on temperature. The governing model equations of a slender glass fiber in the centrifugal spinning process consist of system of nonlinear differential equations with differential constraint in one space dimension (along the arc-length of the fiber center line). Since the derivation of the model follows similar steps to the one employed by the co-author in his studies of isothermal curved fibers (Panda *et al*., , 2008), only brief comments will be made on its derivation.

Neglecting aerodynamic forces, and following the approach in (and scaling (i) the cross-sectional area of the fiber, fluid velocity and temperature by A_o (cross-sectional area of the nozzle), u_o (exit velocity at the nozzle) and T_o (mean temperature of the fluid at the nozzle), and (ii) arc length, time, viscosity and outer force by typical fiber length L_o, melt viscosity μ_o and $\mathbf{f}_o$ (outer force = ($\rho u_o^2 / L_0$)) respectively, the conservation of mass, momentum and heat transfer equations lead to a system of differential equations in non-dimensional form

Then the conservation of mass, momentum and heat transfer equations lead to a system of differential equations in non-dimensional form

$$(Au)' = 0 \tag{1}$$

$$(uAv)' = [(\frac{3}{Re}\mu(T)(Au') + \frac{\sqrt{\pi}\sqrt{A}}{2We})\boldsymbol{\gamma}']' + A\mathbf{f} \tag{2}$$

$$(uAT)' = \frac{1}{Pe}(AT')' - 2\sqrt{\pi}\sqrt{A}(St(T - T_a) + R(T^4 - T_a{}^4)) \tag{3}$$

with:

$$v = u\boldsymbol{\gamma}' \tag{4}$$

and the arc length constraint:

$$\|\boldsymbol{\gamma}'\| = 1 \tag{5}$$

where superscript prime denotes the derivative in respect to the axial coordinate s. We solve the system for $s \in [0, L]$, where L is considered to be a finite length of the fiber. By $\boldsymbol{\gamma}(s) = (\gamma_1, \gamma_2, \gamma_3) \in R^3$ and $v(s) = (v_1, v_2, v_3) \in R^3$, we denote the fiber position and the velocity at s. Additionally, $u(s) \in R$ describes the tangential velocity of a fluid particle moving along the centerline. The symbols $A(s)$ and $T(s)$ denote the cross-sectional area of the fiber and the fluid temperature respectively, at the arc length position s. Also T_a stands for the constant ambient temperature. Finally, Eq. (5) is the condition for the arc-length parametrization of the fiber which is defined by a normalized tangent. Here $\mathbf{f}$ represents the body forces which include the force of gravity and the rotational forces, i.e.,

$$\mathbf{f}(s,t) = \frac{1}{Fr^2}\mathbf{e}_g - \frac{2}{Rb}(\mathbf{e}_{\boldsymbol{\omega}} \times v) - \frac{1}{Rb^2}(\mathbf{e}_{\boldsymbol{\omega}} \times (\mathbf{e}_{\boldsymbol{\omega}} \times \boldsymbol{\gamma})), \tag{6}$$

where $\mathbf{g} = \mathbf{e}_g g$ and $\boldsymbol{\omega} = \mathbf{e}_{\boldsymbol{\omega}}\omega$ are the acceleration due to gravity and the angular velocity of the rotating device. Note that the momentum Eq. (2) takes into account the effects of axial viscous stress (proportional to $1/Re$), gravity $(1/Fr)$, rotational forces $(1/Rb)$ and surface tension $(1/We)$, where non-dimensional parameters

$$Re = L_0\rho u_0/\mu_0, \qquad Rb = u_0/L_0\omega, \qquad Fr = u_0/\sqrt{gL_0}, \qquad We = (\varepsilon L_0/2)\rho u_0^2/\sigma,$$

stand for Reynolds, Rossby, Froude and Weber number, respectively. Similarly in heat transfer Eq. (3) the cooling effects of heat convection, controlled by Stanton number St and heat radiation, proportional to the radiation number R, are included together with the axial heat transfer (proportional to inverse Peclet number Pe):

$$St = \alpha_{ht}/\rho C_p u_0, \qquad R = \alpha_e \sigma_{SB} T_a^3/\rho C_p u_0, \qquad Pe = \rho C_p L_0 u_0/\kappa,$$

where, σ_{SB} is the StefanBoltzmann constant and α_e is the emissivity constant.

For completing the statement of the problem, the corresponding boundary conditions should be added. The first group of boundary conditions follows from the definition of the characteristic scales:

At the nozzle: $(s = 0)$

$$A(0) = 1, \quad u(0) = 1, \quad T(0) = 1, \quad \boldsymbol{\gamma}(0) = \boldsymbol{\gamma}_o, \quad \frac{\partial \boldsymbol{\gamma}}{\partial s}(0) = \boldsymbol{\tau}_o. \tag{7}$$

In the steady case the end of the fiber is not known. However, the highest order derivative of the system equations is second order for the fluid velocity u and temperature T. In addition to the boundary condition at the nozzle Eq. (7) an extra boundary condition is required to close the model equations. Therefore, we imposed the boundary conditions derived through asymptotic reduction for non-isothermal curved jet model at the given length of the fiber. Thus at $(s = L)$ we have:

$$T'(s) = 0. \tag{8}$$

Hence Eq. (3) trivially satisfies for $T = T_a$ at $s = L$. Thus the dynamic boundary condition (Marheineke *et al*., 2009) results as

$$u(L) = \left(1 + L\frac{\sqrt{\pi}}{12}\frac{Re}{We}\frac{1}{\mu(T_a)}\right)^2(L). \tag{9}$$

Moreover, it should be noted that in the unsteady model, neglecting surface tension boundary condition always produces a layer at the end of the cross-sectional area of the fiber, while this will not be observed in the steady model since the model equations will be solved for a given finite length of the fiber.

For our computational purpose we set the configuration shown in Fig. 2 for the rotating device. We consider that the device rotates in the anticlockwise direction along the vector $\mathbf{e}_2$ and the force of gravitation acts in the downward direction. In this case the vectors $\mathbf{e}_g$ and $\mathbf{e}_{\boldsymbol{\omega}}$ of Eq. (6) are equal to $\mathbf{e}_g = (0,-1,0)$ and $\mathbf{e}_{\boldsymbol{\omega}} = (0,1,0)$. By considering the characteristic length to be the radius of the rotating device and fixing origin at the center of the device, the non-dimensional position and direction of the fiber center line at the nozzle are given by $\gamma_O = (1,0,0)$ and $\tau_O = (1,0,0)$, respectively.

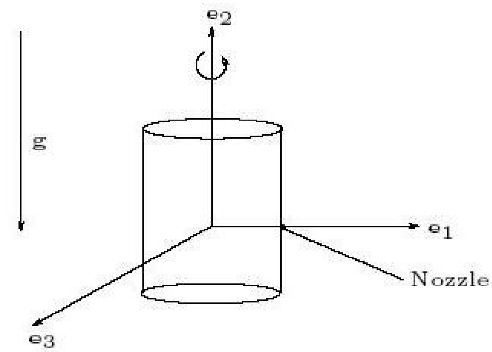

Fig. 2: Schematic diagram of the device showing the directions of rotation and gravity.

The temperature dependence of the fiber viscosity in Eq. (2) is considered in exponential form (Radev *et al*., 2008)

$$\mu(T) = \exp(-k(T-1)), \tag{10}$$

where k is referred as non-dimensional viscosity exponential coefficient, which is scaled by mean temperature T_O. It is to be noted that when $\mu(T) = \mu$ and the fiber is isothermal then temperature Eq. (3) is no more required and model equations reduces to the steady surface tension model of Marheineke *et al*., (2009). Model Eqs. (1)-(4) with boundary conditions Eqs. (7)-(8) are the nonlinear differential equations with differential constraint Eq. (5).

Numerics:

Before we introduce the numerics, we first simplify the equations of the steady-state fiber model. One can consider $\mathbf{v}$ as one of the unknowns of the problem, but for simplicity we eliminate $\mathbf{v}$ from Eq. (4) in order to obtain ordinary differential equations for u and $\boldsymbol{\gamma}$. Furthermore, Eq. (1) provides constant mass flux along the fiber. By using Eq. (7), we get $Au = 1$. Therefore, we can write the equations either in terms of A or u. Indeed, it is helpful to simplify the equations even further by introducing two angles α and β as functions of the arc-length parameter s such that the arc-length constraint Eq. (5) can be expressed as the following differential equation

$$\partial_s\boldsymbol{\gamma} = (\partial_s\gamma_1, \partial_s\gamma_2, \partial_s\gamma_3) = (sin(\alpha)cos(\beta), cos(\alpha), sin(\alpha)sin(\beta)) = \mathbf{e}_{\alpha\beta},$$

with $\alpha(0,t) = \pi/2$ and $\beta(0,t) = 0$. Thus Eq. (2) becomes

$$(u\mathbf{e}_{\alpha\beta})' = [(\frac{3}{Re}\mu(T)(\frac{1}{u}u') + \frac{\sqrt{\pi}}{2We}\frac{1}{\sqrt{u}})\mathbf{e}_{\alpha\beta}]' + \frac{\mathbf{f}}{u} \tag{11}$$

There is variety of discretization techniques available for developing discrete approximations to a set of governing partial differential equations. We apply finite volume method (Versteeg *et al*., 1995, Leveque, 2002) on a staggered grid of uniform cell lengths. Moreover, we again use an up-winding differencing scheme to treat the convective term.

The resulting system of nonlinear discrete equations is solved using the scientific computing program software MATLAB.

RESULTS AND DISCUSSION

The Effects of Heat Radiation and Heat Conduction:

The effect of temperature on the evolution of fibers by varying the cooling factors Peclet number and Radiation number is analyzed in this section. Simulation results of the cross-sectional area, velocity and the temperature of the fiber and fiber geometry are presented.

Fig. 3 shows the effect of Peclet number on non-isothermal solutions; recall that Pe is a measure of specific heat relative to thermal conductivity. Results are shown for the parameters

$Re = 1$, $Fr = 2$, $Rb = 2$, $We = 20$, $k = 1.5$, $St = 0.5$, $R = 0.1$ and $T_a = 0.02$ with varying Peclet number as indicated in the figure caption. All solutions are essentially unchanged with respect to variations of $Pe \geq 10$. Measurable process changes occur in the nonphysical range $1 < Pe < 10$. But a typical spinning process has very high $Pe \approx O(10^3)$. Results clearly demonstrate that the effect of Peclet number very much negligible in the spinning process.

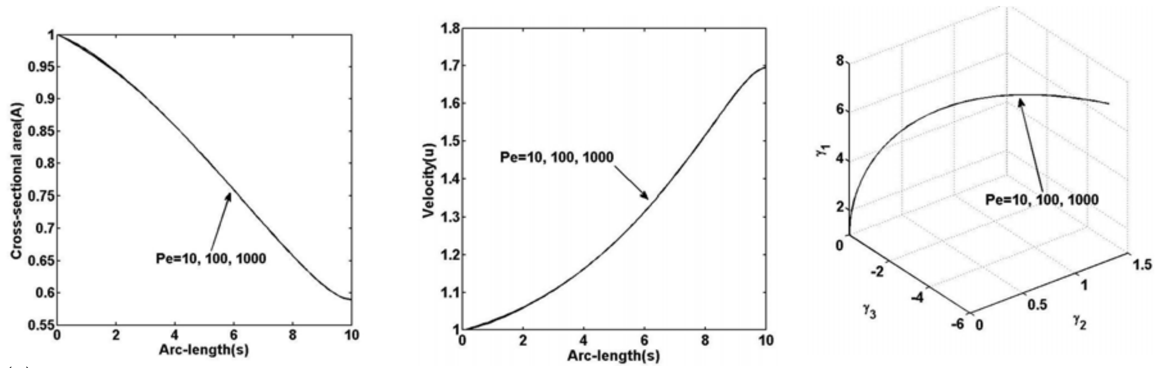

(a) Cross-sectional area (b) Velocity (c) Fiber geometry

Fig. 3: Fiber properties for $\mathrm{Pe} \in \{10, 100, 1000\}$ respectively.

Another cooling factor acting on the fiber is the radiation number R and the effect of heat radiation on the fiber properties demonstrated in Fig. 4. It should be mentioned that the cooling effect of radiation number is less important than the effect of Stanton number.

Simulation results of the cross-sectional area, velocity, and the fiber geometry are presented for three different radiative heat transfer parameter R. The other parameters used in the simulations are $Re = 1$, $Fr = 2$, $Rb = 2$, $We = 20$, $k = 1.5$, $St = 0.5$, $Pe = 1000$ and $T_a = 0.02$.

It is clear from Fig. 4 that the radiative transfer parameter R is insensitive on fiber solutions i.e., the radiative effect is highly negligible.

In Fig. 5 the temperature profile of fiber for different cooling factors is given. With an increase in St (i.e. an increase in the heat-transfer coefficient), keeping the other parameters constant, we observe an increased heat loss at $St = 100$ as compared to $St = 0.01$. In the case of Peclet number same results holds (Fig. 5(b)). But radiative parameter have highly negligible effect on fiber temperature (Fig. 5(c)).

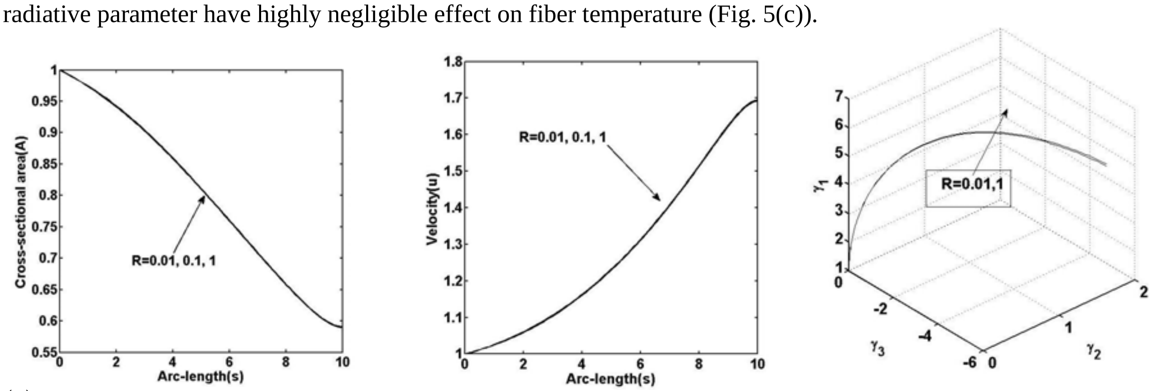

(a) Cross-sectional area (b) Velocity (c) Fiber geometry

Fig. 4: Simulation results for different values of radiation number.

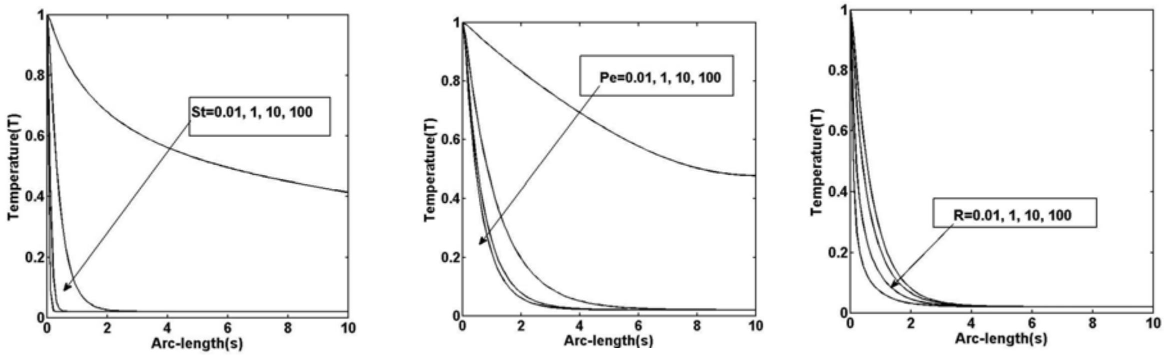

(a) (b) (c)

Fig. 5: Temperature profile of fiber for different cooling factors.

Effect of Heat Transfer Parameter (St):

Taking our observations into account, neglecting conduction and radiation effect, i.e., neglecting conduction and radiation terms in the heat equation (by taking $Pe=\infty$ and $R=0$) our steady model can be simplified. Thus in the simplified model thermal effects on the fiber more depends on the variations of heat transfer parameter St. Fig. 6 exhibits the effect of the heat transfer parameter St, Stanton number on non-isothermal solutions and the other parameters used in the simulation are $Re=1,\ Fr=2,\ Rb=2,\ We=20,\ k=1.5,\ Pe=100,\ R=0.1$ and $T_a=0.02.$

The fiber center-line is plotted in Fig. 6(d) against Stanton number. To see it more clearly, a projection of the three-dimensional center-line is plotted in the Fig. 6(c) onto the (γ_3,γ_1) plane. It is observed that the Stanton number changes significantly the dynamics of fiber center-line. Figure further suggests that a cooler ambient results in a more oriented fiber. When Stanton number increases, the temperature in the fiber decreases rapidly and fiber center-line becomes more coiled. Physically this implies that with decreasing temperature the viscosity of the fiber increases and, consequently, center-line with high viscosity has a larger curvature. This model prediction is consistent with industrial experience. Also for higher Stanton number there is an immediate decrease of area of cross-section of fiber near the orifice due to the convective cooling (Fig. 6(a)). This results in a fiber that becomes thinner near the orifice and accordingly the velocity increases faster near the orifice (Fig. 6(b)). It can be easily seen from Eq. (9) that, the final velocity is bounded above by

$$u(L) \le u(0) + \int_0^L \left(\frac{\sqrt{\pi}}{6} \frac{Re}{We} \frac{1}{\mu(T)} \right)^2 ds$$

and it depends on temperature.

It is also important to see the influence of viscosity exponential coefficient k which influences the viscous effect on the fiber. The results on temperature of the fiber for a different viscosity exponential coefficients $k\in\{1,2\}$ when $Re=1,\ Fr=2,\ Rb=2,\ We=20,\ St=0.5,\ Pe=1000$, and $T_a=0.02$ are given in Fig. 7. From the exponential dependency between viscosity and temperature (see Eq. (10)) we have the obvious result that for higher temperature there is an exponential decrease in the viscosity. Also it is to be noted that there is an inverse proportionality between the viscosity exponential coefficient (k) and viscosity. We can conclude that the higher values of viscosity exponential coefficient makes an increase in the temperature on the fiber.

Further we could simplify the problem using the temperature monotonicity in stationary flow, thereby we could cast the governing equations in an analytically and numerically advantageous form. From the results it is to be observed that temperature profile is a monotonically decreasing function with respect to s (this statement is true till no crystallinity occurs). Consequently the viscosity field can be treated as a function of axial length s. Thus, $1/T$ increases with s and can be written in the form (Perera, 2009) $1/T=C_1 s+C_2$ for some constants C_1 and C_2. Using the boundary condition $T(0)=1$, we get, $C_2=1$ and C_1 is still unknown constant parameter. It may be noted that if conduction effect is taken into account the constant C_1 coincides with a value $C_1=(1/L)((1/T_a)-1)$ for a finite length L of fiber.

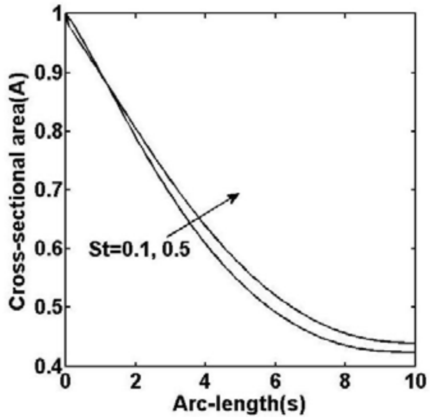

(a)

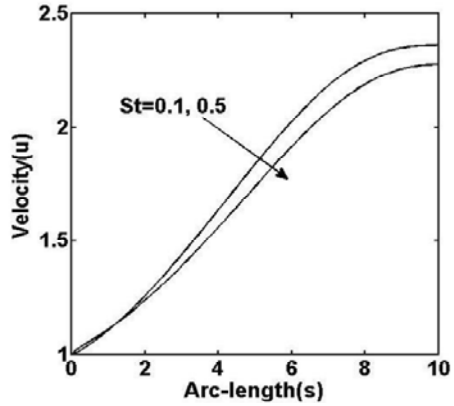

(b)

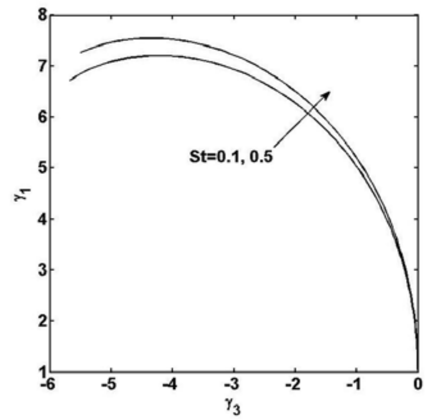

(c) **Fiber geometry** 2D

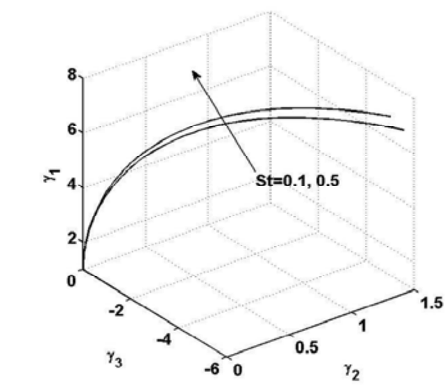

(d) **Fiber geometry** 3D

Fig. 6: Fiber properties for $\mathrm{St} \in \{0.1, 0.5\}$ respectively.

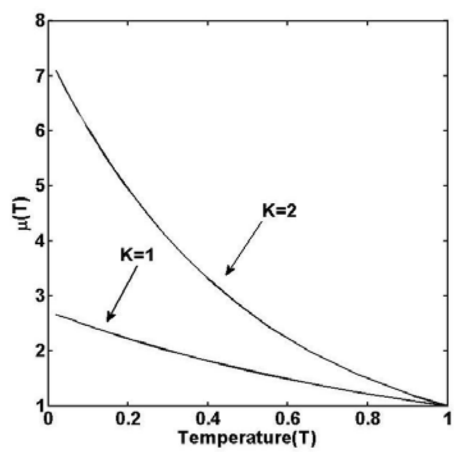

Fig. 7: Temperature versus $\mu(T)$.

Fig. 8 exhibits the comparison results for the heat transfer parameter St and the constant C_1. from the figure it is clear that for a typical value of $St = 0.5$ the temperature profile coincides for a value in neighborhood of $C_1 = 3.8$.

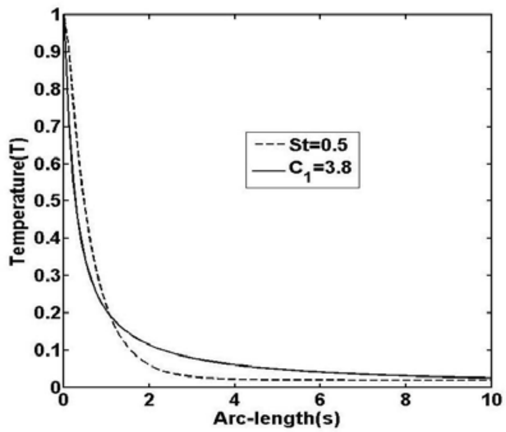

Fig. 8: Comparison of the parameter St in the temperature equation $(T)' = -2\sqrt{\pi}\sqrt{A}(St(T-T_a)+R(T^4-T_a^4))$ with the parameter C_1 in the simplified heat equation $1/T = C_1 s + C_2$

Conclusion and Outlook:

In this paper we carried out a detailed study on the effects of temperature, which are coupled to the dynamics of fibers via the strongly temperature-dependent viscosity. As a consequence important fiber dynamics and cooling aspects of the problem are discussed. Numerical results for the fiber cross-sectional area, axial velocity, temperature and fiber geometry are shown, which illustrates the cooling effects of Stanton number, Peclet number, Radiation number, Reynolds number, Weber number and Rossby number. Results show that the findings have a greater significance when the fluid model is non-isothermal. Variations in cooling parameters results in the variations of curvature of center-line of the fiber i.e., fiber center-line becomes more coiled for higher Stanton numbers due to the viscous domination. For Peclet number the measurable process changes occur only in the nonphysical range $(1 < Pe < 10)$. The radiative effect is highly negligible on the fiber dynamics. Also shown the results for simplified model to validates our findings. Further we could simplify the problem using the temperature monotonicity in stationary flow, thereby we could cast the governing equations in an analytically and numerically advantageous form. However, for the realistic simulation of the glass fiber model, many other phenomena like aerodynamics effects and Non-Newtonian rheology should be taken in account in the future work.

ACKNOWLEDGEMENT

The second author is grateful to National Institute of Technology, Calicut for the financial grant received under FRG No. FRG/08-01 of Dt. 27-11-2008.

REFERENCES

Arridge, R.G.C. and K. Prior, 1964. Cooling time of silica fibers. Nature, 203: 386-387.

Bechtel, S.E., M.G. Forest and Q. Wang, 1992. Non-isothermal modeling of fiber spinning. Recent Adu. Non-Newtonian Flow PED-141, 37.

Bourne, D.E. and H. Dixon, 1971. The cooling of fibers in the formation process. Int. J. Heat Mass Transfer, 24: 1323-1332.

Chida, K. and Y. Katto, 1976. Conjugate heat transfer of continuously moving surfaces. Int. J. Heat Mass Transfer, 19: 461-470.

Cummings, L.J. and P.D. Howell, 1999. On the evolution of non-axissymetric viscous fibers with surface tension inertia and gravity. Jr. Fluid. Mech., 389: 361-389.

Decent, S.P., M. Simmons, E. Parau, D. Wong, A. King and L. Partridge, 2004. Liquid jets from a rotating orifice. In Proceedings of the 5th In- ternational Conference on Multiphase Flow, ICMF' 04, Yokohama, Japan.

Decent, S., A. King and I. Wallwork, 2002. Free jets spun from a prilling tower, J. Eng Math, 42: 265-282.

Dewynne, J., J.R. Ockendon and P. Wilmott, 1989. On a mathematical model for fiber tapering. SIAM Jr. App. Math., 49(4): 983-990.

Dewynne, J.N., P.D. Howell and P. Wilmott, 1994. Slender viscous fibers with inertia and gravity. Quart Jr. of Mech. and Appl. Math., 47: 541-555.

Doyle, P.J., 1994. Glass Making Today. R.A.N. Publishers, Ohio.

Eggers, J., 1997. Nonlinear dynamics and breakup of free surface flows. Rev. Mod. Phy., 69(3).

Forest, M.G. and H. Zhou, 2001. Unsteady analysis of thermal glass fiber drawing processes. Euro. Jr of Applied Mathematics, 12: 479-496.

Geyling, F.T., 1976. Basic fluid dynamic considerations in the drawing of optical fibers. Bell Syst. Tech. J., 55: 1011-1056.

Glickman, L.R., 1968. The cooling of glass fibers. Glass Techn., 9(5): 131-138.

Gotz, T., A. Klar, A. Unterreiter and R. Wegener, 2008. Numerical evidence for the non-existence of stationary solutions of the equations describing rotational fiber spinning. Mathematical Models and Methods in Applied Sciences, 18(10): 1829-1844.

Gupta, G. and W.W. Schultz, 1998. Non-isothermal flows of Newtonian slender glass fibers. Int. Jr. Non-Linear Mechanics., 33(1): 151-163.

Hlod, A., A.C.T. Aarts, V.D. Ven, A.A.F. and M.A. Peletier, 2007. Mathematical model of falling of a viscous jet onto a moving surface. European Journal of Applied Mathematics, 18: 659-677.

Hlod, A., 2009. Curved jets of viscous fluid: Interactions with a moving wall. PhD thesis, Eindhoven University of Technology.

Huynh, B.P. and R.I. Tanner, 1983. Study of the non-isothermal glass fibre drawing process. Rheol. Acta., 22: 482.

Kaye, A., 1999. Convected coordinates and elongational flow. Jr. Non-Newtonian Fluid Mech., 40: 55-77.

Kase, S. and T. Matsuo, 1965. Studies on melt spinning: Fundamental equations on the dynamics of melt spinning. Jr. of Poly. Sc. Part-A, 3: 2541-2554.

Kolk, E., 2005. Mathematical models for a rotor spinning process. Interim report, TU Delft.

Leveque, R.J., 2002. Finite Volume Methods for Hyperbolic Problems. Cambridge University Press.

Maddison, R. and P.W. Mcmillan, 1978. The cooling rate of glass fibers. Glass Technology, 19(5): 127-129.

Marheineke, N. and R. Wegener, 2009. Dynamics of curved viscous fibers with surface tension. Jr. Fluid Mech., 622: 345-369.

Matovich, M.A. and J.R.A. Pearson, 1969. Spinning a molten thread line. Ind. Eng. Chem. Fundamen., 8(4): 605-609.

Panda, S., 2006. The Dynamics of Viscous Fibers. PhD thesis, Technische Universitat Kaiserslautern.

Panda, S., R. Wegener and N. Marheineke, 2007. The dynamics of curved viscous fibers. Industrial mathematics at ECMI, 2006: 685-690, Springer.

Panda, S., R. Wegener and N. Marheineke, 2008. Systematic derivation of an asymptotic model for the dynamics of curved viscous fibers. Math. Meth. Appl. Sci., 31: 1153-1173.

Perera, S.S.N., 2009. Viscoelastic Effect in the Non-Isothermal Melt Spinning Processes. Applied Mathematical Sciences, 3(4): 177-186.

Radev, S.P., T.L. Boyadjiev and F. Onofri, 2008. Mathematical modeling of a steady glass fiber drawing process. All Russian Semianar on Aerohydrodinamics ded- icated to the 90-th Anniversary of S.V. Vallander, St. Petersburg University, February 5-7, Russia, 7 pages.

Schultz, W.W. and S.H. Davis, 1982. One-dimensional liquid fibers. Jr. Rheol., 26: 331-345.

Shah, Y.T. and J.R.A. Pearson, 1972. On the stability of nonisothermal fiber spinning. Ind. Eng. Chem. Fundam, 11(2): 145-149.

The Math Works, 2007. Inc. Matlab R2007b Documentation.

Versteeg, H.K. and W. Malalasekera, 1995. Introduction to Computational Fluid dynamics: The Finite Volume Method, Longman.

Wang, Q. and G.M. Forest, 1994. Numerical simulations of non-isothermal fiber spin ning processes. Numer. Methods Non-Newtonian Fluid Dynamics FED-179: 11-20.

Wallwork, I.M., S.P. Decent, A.C. King and F.R.S. Schulke, 2002. The trajectory and stability of a spiraling liquid jet. Part 1. Inviscid theory, Jr. Fluid. Mech., 459: 43-65.